Paper

Geometrical and Topological Features of Isotrigon Textures

Yoshinori Nagai[1] and Ted Maddess[2]

(Received 20 January 2010, Revised 25 January 2010)

Abstract: Isorigon textures are considered from the perspectives of geometry and topology. The textures considered here consist of finite size pixels. Thus we should use discrete mathematics. We use the Gaussian and mean curvatures to characterize textures by introducing the discrete scheme of curvature calculation from our previous work (*Mem. Cntr. Infor. Sci. Kokushikan U* **30** (2009) 1–13). We also consider Minkowski functionals using the morphological analysis of images, one of which comes from the application of the Gauss-Bonnet theorem on closed oriented surfaces. This idea is an intrinsic property of surface so that the application of Gauss-Bonnet theorem leads to the topology of surfaces. In the topology of surfaces integrated Gaussian curvature plays a key role. Thus the integrated Gaussian curvature of surfaces consisting of finite size elements is calculated for isotrigon textures. The integrated Gaussian curvature has large values for isotrigon textures and we discuss why this occurs.

1. Introduction

The brightness levels of two dimensional textures can be interpreted as the height of a surface that can be understood in terms of the geometric features of the surface. Our study involves attempting to understand isotrigon textures consisting pixels of two or three coloring in terms of geometric features. The isotriogon textures have discrete elements and so are properly described by discrete mathematics. Thus we have utilized a Gauss-Bonnet scheme of covering the texture surface by polygons. Hyde, S. T. gave formulae for the Gaussian and mean curvatures from which it is easy to obtain a discretized scheme of Gaussian and mean curvatures of a patch-worked surface of small polygons [1, 2]. Thus we have previously derived Gaussian and mean curvatures of brightness surfaces of textures in a previous work [3].

In the present paper, we concentrate seeing the features of ternary isotrigon textures to discover if there is a role for hyperbolicity, i.e., negative curvature effects. Textures comprised of three levels of brightness have the lowest required number of states to form negative curvature structures for patch-work surfaces. The results of applying curvature concepts to several kinds of isotrigon textures showed that zero Gaussian curvature ($K = 0$) can yield a discrimination index for isotrigon textures and mean curvature distribution of an isotrigon texture follows the texture's own pattern. Here we present the case of isotrigon textures using one of 24 modulo 3 rules all of which generate isotrigon textures [4]. The modulo 3 cellular automata rules parsimoniously describe isotrigon textures. These results are shown in Section 2.

Binary images including textures have been investigated from the topological viewpoint [5]. In particular image morphology has been analyzed using so-called Minkowski functionals [5, 6]. The idea of Minkowski functionals is strictly related to Gauss-Bonnet theorem for global surface

[1] Center for Information Science, Kokushikan University, 4–28–1 Setagaya, Setagaya-ku, Tokyo 154–8515, Japan
[2] Center of Excellence in Vision Sciences and Center for Visual Science, Research School of Biology, Australian National University, Canberra ACT 0200, Australia

property [6, 7, 8]. Integrated Gaussian curvature of a closed surface has topological invariance in homeomorphism [7]. The polygonal network on the closed surface yields the idea that the integrated Gaussian curvature is equivalent to Euler characteristics [6]. The above facts have been used to form the Minkowski functionals in image morphology analysis [5, 6]. Here the integrated curvatures are calculated for isotrigon textures. In this study, integrated curvatures are given by summing up over covering local squares consisting of five pixels. These results are shown in Section 3.

The integrated curvatures presented in this paper are very large values. So these large values will be discussed in section 4. The global Gauss-Bonnet theorem is significant for smooth surface, but our study of curvature is discrete scheme. Thus there exist singular lines and points on the texture surface. These points should be studied in discrete surface viewpoints. This field is not completed in the mathematical studies.

2. Curvatures of Ternary Isotrigon Textures

The textures investigated here consist of discrete pixels. We choose each pixel to form a square so that the brightness surface around the considered pixel is a four sided pyramid. The curvature for the top or bottom of the four sided pyramid is defined using Hyde's results [1, 2]. The Gaussian (K) and mean curvatures (H) are as follows [3],

$$K = \frac{6\left(2\pi - \sum_{(j,k)} \tan^{-1}\left(\dfrac{\sqrt{1+\dfrac{\Delta I_j^2+\Delta I_k^2}{a^2}}}{\dfrac{\Delta I_j \Delta I_k}{a^2}}\right)\right)}{a^2 \sum_{(j,k)} \sqrt{1+\dfrac{\Delta I_j^2+\Delta I_k^2}{a^2}}} \tag{1}$$

$$H = -\frac{3}{2} \frac{\sum_j \dfrac{\Delta I_{j-1}+\Delta I_{j+1}}{\left|\Delta I_{j-1}+\Delta I_{j+1}\right|} \sqrt{1+\dfrac{\Delta I_j^2}{a^2}} \tan^{-1} \sqrt{\dfrac{\left(1+\dfrac{\Delta I_{j-1}^2+\Delta I_j^2}{a^2}\right)\left(1+\dfrac{\Delta I_j^2+\Delta I_{j+1}^2}{a^2}\right)}{1+\dfrac{\Delta I_j^2-\Delta I_{j-1}\Delta I_{j+1}}{a^2}} - 1}}{a \sum_{(j,k)} \sqrt{1+\dfrac{\Delta I_j^2+\Delta I_k^2}{a^2}}} \tag{2}$$

where a refers to the distance between two neighboring pixel centers, ΔI signifies the brightness of each pixel. In the previous paper [3], we gave the above formulae and the second neighbor vertices Gaussian and mean curvatures, but for the mean curvatures in our previous paper we dropped a sign term. The correct formulae are presented in the Appendix of this paper.

The curvature formulae for a discritized scheme (eq.1 and eq.2) are applied to so-called isotrigon textures. The investigated isotrigon textures are five classes of three colored textures, namely, Random, Box, Cross, Oblong, and Zigzag. Fig.1 shows examples of ternary textures, and the

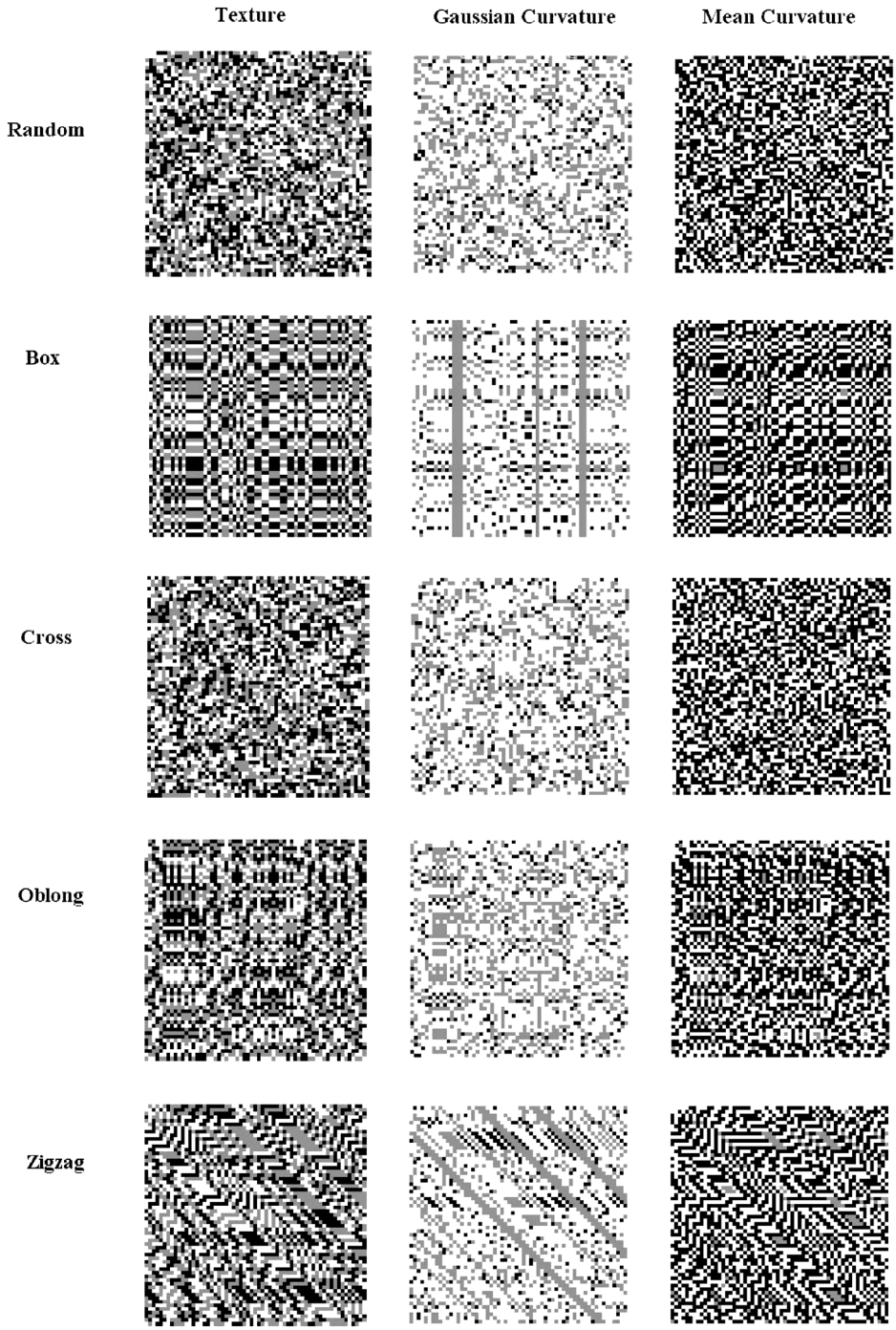

Fig. 1 Examples of Isotrigon textures and their Gaussian and mean curvature distributions. The calculated curvature values are given for 5 classes of ternary isotrigon textures, i.e., Random, Box, Cross, Oblong, and Zigzag. The curvature values are discritized to three levels, these are negative (color black), zero (color grey), and positive (color white). In Gaussian curvature, the distribution $K = 0$ implies sparse features that allow recognition of the texture classes, especially Box and Zigzag. The mean curvature distribution tends follows the original busy texture structure

Gaussian and mean curvature distributions of corresponding textures for these five classes. In Fig.1, the curvature values for each pixel are discritized into three levels, i.e., -1 for negative values, 0 for zero, and $+1$ for positive values. In the present study, the cellular automata rules used for making the isotrigon ternary textures had a modulo 3 form,

$$S_d = f(S_a, S_b, S_c) = (S_a - S_b + S_c)_{\mathrm{mod}3} \quad , \tag{3}$$

where S_a, S_b, S_c, $S_d \in \{-1, 0, 1\}$. There are 24 modulo 3 rules that produce isotrigon textures. The reason we selected the above rule is that the rule generates well structured textures using Box, Oblong, and Zigzag gliders that are similar in appearance to binary isotrigon textures made by using these gliders. The procedure for applying this rule for these gliders classes is shown in Fig. 2. In the picture presentation of Fig. 1, the logic of the pixel colorings was white for $+1$, grey for 0, and black for -1, following the definition of visual contrast.

As seen from Fig. 1, the tree-color mean curvature map mimics the texture appearance. Long grey lines appeared in the Gaussian curvature maps of the Box and Zigzag textures, namely, vertical grey line in Box texture and diagonal grey line in Zigzag texture. These facts imply that the Gaussian curvature distribution should supply some quantity to discriminate features representing the isotrigon texture classes. that is to say the Gaussian curvature map seems to extra a sparse set of features that are the recognizable components of the textures.

Mean percent curvature statistics are tabulated in Table 1. The obtained statistics of percentage content of Gaussian and mean curvature values can be compared with the local square configuration that gave estimates of curvature signs in previous paper [3]. These percentages are shown in Tables 2, 3, and 4. The percentage of curvature values $K=0$, $H=0$, and $H\neq 0$ are within admissible range, but that of $K<0$ and $K>0$ are different to each other. These value differences will be

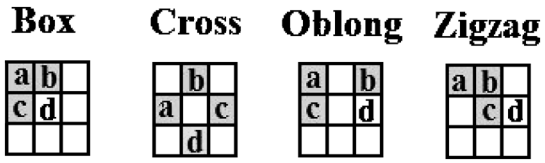

Fig. 2 Rule (eq.3) application procedure for texture classes of Box, Cross, Oblong, and Zigzag. The three variables (a, b, c) of each 3 by 3 pixel glider determine the state of pixel d using the rule described with eq.3

Table 1 Gaussian and Mean Curvatures Statistics of Random Texture and Four Isotrigon Textures

Texture	$K<0$	$K=0$	$K>0$	$H=0$	$H\neq 0$
Random	8.09%	27.72%	64.18%	3.69%	96.31%
Box	8.62%	28.39%	62.99%	5.63%	94.37%
Cross	8.46%	28.48%	63.06%	3.81%	96.19%
Oblong	8.45%	28.62%	62.93%	3.82%	96.18%
Zigzag	8.19%	29.20%	62.61%	3.69%	96.31%

The statistic calculations were performed for the texture sizes 20, 40, 60, 80, and 100 pixels square. For each texture class and each texture size, five example textures were generated and we counted the curvatures that had positive, zero, and negative values. The percentages are obtained by dividing each count by the number of pixels. These values are not so different in each texture size so that we averaged over all sizes.

Table 2 Theoretical expectation of Curvature statistics

K<0, H=0		K=0, H=0		K>0, H=0	
0	0%	11	4.53%	0	0%
K<0, H≠0		K=0, H≠0		K>0, H≠0	
46	18.93%	52	11.52%	134	55.14%

The percentage of positive, zero, and negative values are calculated based on previous work [3]. Since we had errors of classification in previous work, we correct and count the contributing numbers tabulate the results here.

Table 3 Theoretical expectation for three level classification of Gaussian curvatures

K<0		K=0		K>0		Total	
46	18.93%	63	25.92%	134	55.14%	243	100%

The expectation values come from Table 2.

Table 4 Theoretical expectation for the zero or not zero classification of mean curvatures

H=0		H≠0		Total	
11	4.53%	232	95.47%R	243	100%

discussed in Section 4.

3. Global Gauss-Bonnet Theorem and Minkowski Functionals

The application of the Gauss-Bonnet theorem to a closed surface leads to the topological nature of inner surface characteristics. Following Kreyszig [7], applying the Gauss-Bonnet theorem to a theorem of closed surfaces becomes follows.

The Gauss-Bonnet theorem (theorem 54.1, p.169 of ref. 7) is written as,

$$\int_C \kappa_g ds + \iint_S K dA = 2\pi , \tag{4}$$

where, C denotes the boundary, κ_g geodesic curvature, S a simply connected portion of a surface, and dA the element of area of surface. This gives following theorem (theorem 55.1, p.172 of ref. 7)

$$\iint_S K dA = 4\pi(1-p) \tag{5}$$

where, S is closed orientable surface of genus p. In the proof of above theorem (pp. 172–174 of ref. 7), the following relation is presented,

$$4p\pi(1-\frac{1}{2p}) + \iint_S K dA = 2\pi . \tag{6}$$

The text book by Guggenheimer (p. 286 ref. 8) gives the relation between integrated Gaussian curvature and the Euler characteristic (also Euler index or Euler number), namely,

$$\iint KdA = 2\pi(V - E + F) = 2\pi\chi\,. \tag{7}$$

Thus we obtain relation between Euler index and genus as follows,

$$\chi = V - E + F = 2(1 - p)\,. \tag{8}$$

In their morphological analysis of black and white images Michielsen and De Raedt present V, E, and F in the above relation (eq.8) as describing them as Minkowski functionals [5, 6]. Their approach to those images is related to spin-spin interactions. They gave a computational calculation method to obtain the quantities V, E, and χ. Our study here yields χ as the integrated Gaussian curvature, strictly the summation for a discrete scheme of Gaussian curvatures over the covering

Table 5 Integrated curvatures of isotriogon textures

Class	$\sum_A K_A$	$\sum_A H_A$	Estimated χ
Random	1821.51 ± 29.14	-486.71 ± 73.19	580 ± 9
Box	1732.76 ± 118.99	-463.63 ± 120.28	554 ± 40
Cross	1839.73 ± 39.38	-456.55 ± 38.00	586 ± 13
Oblong	1839.30 ± 68.02	-455.98 ± 77.21	585 ± 22
Zigzag	1939.14 ± 61.36	-462.84 ± 68.43	617 ± 19

We used 80×80 pixel textures. Each value is average for 5 texture samples for each texture class. The local square for covering a texture consists of 5 pixels as shown in Fig. 3. Thus the covered area is somewhat smaller than the original texture. Total number of local squares for each texture was 3160.

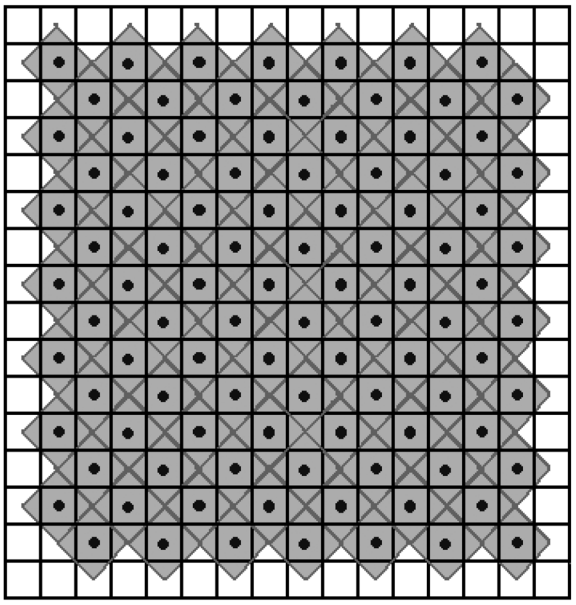

Fig. 3 The covering scheme of a texture. In order to calculate integrated curvature, we should cover a texture with no overlaps and no apertures. This picture schematically shows the covering procedure for a texture using a local configuration of 5 pixel squares. The dots denote pixels where curvature is calculated

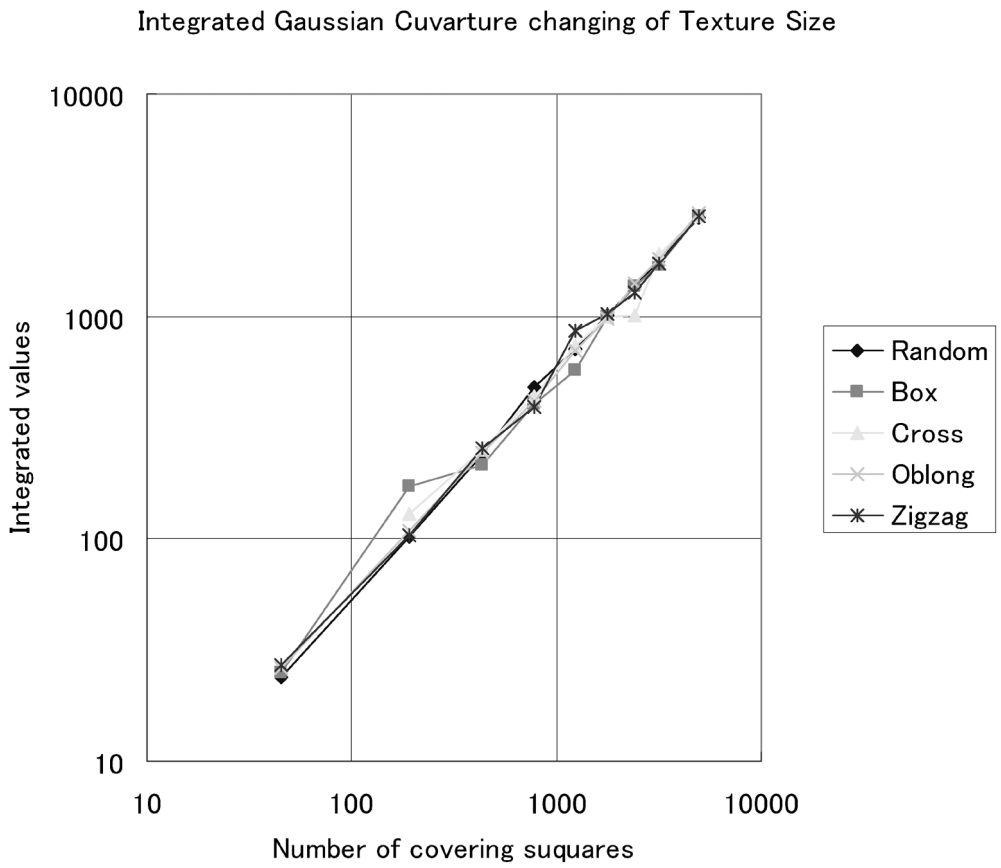

Fig. 4 Dependency of integrated Gaussian curvature on texture size. The integrated Gaussian curvatures are calculated using the covering method shown in Fig. 3. Only one example is calculated for each size. This plot is performed for the number squares covering the textures. Both axes are represented logarithmically

squares of a texture. We also calculate integrated mean curvatures of discrete scheme. Those are tabulated in Table 5.

In Fig. 3 we show the manner of covering a texture with a unit square consisting of 5 pixels (the small grey coloring square in the figure). As easily known from Table 5, the integrated curvatures of Gaussian and mean become large numbers. These points are discussed in section 4. The data of table are obtained as the average of 5 samples of 80×80 pixel textures. We present the dependence of these quantities upon texture size in Figs. 4 and 5. Fig. 4 presents the integrated Gaussian curvatures and Fig. 5 the integrated mean curvatures. These integrated curvatures linearly depend on the contributing pixel numbers to cover a texture, and parabolic dependence on texture size.

4. Discussions

Two points are discussed here. The first is that theoretical number of $K<0$ pixels is larger than actually counted number, while the theoretical number of $K>0$ pixels is smaller than actually counted. Our previous classification of brightness level configurations of pixels to calculate the cur-

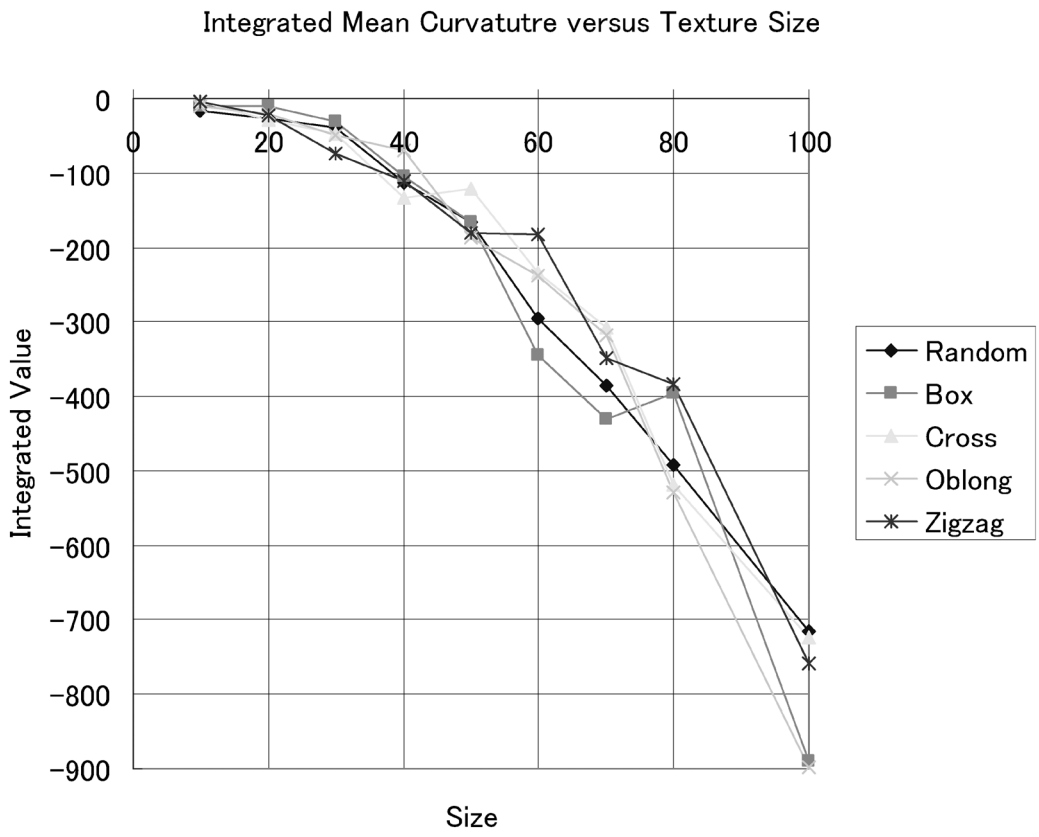

Fig. 5 Dependency of integrated mean curvature on texture size. The values of integrated mean curvatures are plotted against texture size. Usually the integrated mean curvatures take negative values. The dependency is as the square of size, i.e., parabolic. This figure was plotted only using one example for each texture size. The value of integrated curvature has somewhat large fluctuation. So in some cases the deviations become larger

vatures had errors[3]. The present correction gives the theoretical values of the curvature statistics of the present paper. The actually counted value for $H=0$ is a little bit smaller than theoretical prediction. This may be caused by numerical errors for flat plane, i.e., $H=0$ and $K=0$. Since the numerical error gives a very small positive value, the percentage value of $K>0$ accumulates to 0.6 or 0.7%. However this cannot explain our results. Thus we should reconsider the classification of pixel configurations to curvature features.

The second point is that the values of the integrated curvatures are large. If the square surface varies smoothly, the Euler index comes to have the value 1. This implies that the integrated curvature of K becomes 2π. In table 5 we tabulate the estimated Euler indices χs, that were in the range from 550 to 620. Our curvature calculation includes the variables the distance a and brightness level ΔI. Practically speaking, the ratio $\Delta I/a$ and a. In this study we chose $a=1$ and $\Delta I=1$. If a becomes a larger value, the integrated Gaussian curvature becomes smaller. This means we should consider at what scale we should examine the textures. Let a texture T having small half spheres. When we look at this texture T at microscopic scale viewing distances, it approximately becomes a surface composed of many small half spheres. Each small half sphere has Euler index 1 so that the integrated Gaussian curvature is the number of half spheres. Thus we see a large value of integrated Gaus-

sian curvature. If we see this texture at large viewing scale, the small spheres become wrinkles. In this case the integrated Gaussian curvature becomes 1, that is at this scale the surface is equivalent to a square sheet. Following this consideration, at small scale viewing a isotrigon texture of 80×80 size can be divided into 500 or 600 local areas, each area having about 10 pixels.

References

[1] Hyde, S.T., Ninham, B.W., and Zemb, T., Phase boundary for ternary microemulsions. Predictions of a Geometric Model. *J. Phys Chem*, **93** (1989) 1464–1471.

[2] Hyde, S.T., Barnes, I.S., and Ninham, B.W., Curvature energy of surfactant interfaces confined to the plaquettes of a cubic lattice. *Langmuir*, **6** (1990) 1055–1062.

[3] Nagai Y., Hyde S.T., Maddess T., Geometrical characterization of textures consisting of two or three discrete colourings. *Mem Cntr Info Sci. Kokushikan U* **30** (2009) 1–13.

[4] Maddess, T., Nagai, Y., James, A. C., Ankiewicz, A., Binary and ternary textures containing higher-order spatial correlations, *Vision Res.* **44** (2004) 1093–1113.

[5] Michielsen, K., De Raedt, H., Integral-Geometry Morphological Image Analysis, *Physics Report* **347** (2001) 461–538.

[6] Michielsen, K., De Raedt, H., Morphological Image Analysis, *Comp. Phys. Comm.* **132** (2000) 94–103.

[7] Kreyszig, E., *Differential Geometry*, Dover, New York (1991).

[8] Guggenheimer, H. W., *Differential Geometry*, Dover, New York (1977).

Appendix

In our previous work on geometry of texture [3], we dropped the sign term for the mean curvature, eqs.2.9 and 2.11. We show the correct expression of mean curvatures for nearest and second nearest configurations below.

$$H = -\frac{3}{2}\frac{\displaystyle\sum_j \frac{\Delta I_{j-1}+\Delta I_{j+1}}{\left|\Delta I_{j-1}+\Delta I_{j+1}\right|}\sqrt{1+\frac{\Delta I_j^2}{a^2}}\,\tan^{-1}\sqrt{\frac{\left(1+\dfrac{\Delta I_{j-1}^2+\Delta I_j^2}{a^2}\right)\left(1+\dfrac{\Delta I_j^2+\Delta I_{j+1}^2}{a^2}\right)}{1+\dfrac{\Delta I_j^2-\Delta I_{j-1}\Delta I_{j+1}}{a^2}}-1}}{a\displaystyle\sum_{(j,k)}\sqrt{1+\frac{\Delta I_j^2+\Delta I_k^2}{a^2}}} \tag{A.1}$$

$$H = -\frac{3}{4}\frac{\displaystyle\sum_j \frac{\Delta I_{j-1}+\Delta I_{j+1}}{\left|\Delta I_{j-1}+\Delta I_{j+1}\right|}\sqrt{1+\frac{\Delta I_j^2}{2a^2}}\,\tan^{-1}\sqrt{\frac{\left(1+\dfrac{\Delta I_{j-1}^2+\Delta I_j^2}{2a^2}\right)\left(1+\dfrac{\Delta I_j^2+\Delta I_{j+1}^2}{2a^2}\right)}{1+\dfrac{\Delta I_j^2-\Delta I_{j-1}\Delta I_{j+1}}{2a^2}}-1}}{a\displaystyle\sum_{(j,k)}\sqrt{1+\frac{\Delta I_j^2+\Delta I_k^2}{2a^2}}} \tag{A.2}$$